

NANO EXPRESS

Open Access

Investigation on the passivated Si/Al₂O₃ interface fabricated by non-vacuum spatial atomic layer deposition system

Shui-Yang Lien¹, Chih-Hsiang Yang², Kuei-Ching Wu³ and Chung-Yuan Kung^{2*}

Abstract

Currently, aluminum oxide stacked with silicon nitride (Al₂O₃/SiN_x:H) is a promising rear passivation material for high-efficiency P-type passivated emitter and rear cell (PERC). It has been indicated that atomic layer deposition system (ALD) is much more suitable to prepare high-quality Al₂O₃ films than plasma-enhanced chemical vapor deposition system and other process techniques. In this study, an ultrafast, non-vacuum spatial ALD with the deposition rate of around 10 nm/min, developed by our group, is hired to deposit Al₂O₃ films. Upon post-annealing for the Al₂O₃ films, the unwanted delamination, regarded as blisters, was found by an optical microscope. This may lead to a worse contact within the Si/Al₂O₃ interface, deteriorating the passivation quality. Thin stoichiometric silicon dioxide films prepared on the Si surface prior to Al₂O₃ fabrication effectively reduce a considerable amount of blisters. The residual blisters can be further out-gassed when the Al₂O₃ films are thinned to 8 nm and annealed above 650°C. Eventually, the entire PERC with the improved triple-layer SiO₂/Al₂O₃/SiN_x:H stacked passivation film has an obvious gain in open-circuit voltage (V_{oc}) and short-circuit current (J_{sc}) because of the increased minority carrier lifetime and internal rear-side reflectance, respectively. The electrical performance of the optimized PERC with the V_{oc} of 0.647 V, J_{sc} of 38.2 mA/cm², fill factor of 0.776, and the efficiency of 19.18% can be achieved.

Keywords: PERC; Non-vacuum spatial atomic layer deposition; Al₂O₃/SiN_x:H stacked rear passivation; Blister; Triple-layer SiO₂/Al₂O₃/SiN_x:H stacked passivation films

Background

For the past decade years, dielectric films have become promising materials applied in high-efficiency silicon solar cells due to their superior surface passivation effect. An attractive candidate for outstanding Si surface passivation is aluminum oxide (Al₂O₃), which can be deposited by physical vapor deposition (PVD) system [1], chemical vapor deposition (CVD) system [2-4], liquid-phase deposition (LPD) technique [5,6], and atomic layer deposition (ALD) system [7-9]. Generally, ALD system is the most suitable choice for the deposition of Al₂O₃ owing to some advantages: (i) capable of producing very thin conformal and uniform films, (ii) with large process temperature window, and (iii) able to deposit films on high-aspect-ratio substrates. However, traditional plasma-

assist ALD and thermal ALD have an extremely low deposition rate of the order of dozen picometers per second; the industrial application of this technique is chiefly limited to CMOS and DRAM processes [10]. Recently, Al₂O₃ films are applied to a noted cell structure so-called passivated emitter and rear cell (PERC) as the passivation layers. The PERC structure which offers the possibility of importantly improved performance over traditional commercial cell design needing only little extra process steps can achieve the efficiency of around 22%. Hence, the PERC structure is going to be the next key product of most solar companies.

For the solar industrials, the deposition of Al₂O₃ for PERC is mainly by turn-key plasma-enhanced chemical vapor deposition (PECVD) technique due to its higher production capacity in comparison with ALD system. But the uniformity of the PECVD Al₂O₃ films is difficult to control well, making the film thicker at the central region and thinner around the edge of the wafer. A

* Correspondence: cykung@dragon.nchu.edu.tw

²Department of Electrical Engineering, National Chung Hsing University, 250 State Road, Taichung 402, Taiwan

Full list of author information is available at the end of the article

spatial-type ALD with both merits of a high deposition rate and producing films with a high-level uniformity has been proposed to provide a great passivation effect and enhance the production capacity. The precursor TMA ($\text{Al}(\text{CH}_3)_3$) and reactant water vapor (H_2O) were used to proceed two half reactions to deposit the Al_2O_3 films in spatial ALD. A little amount of hydrogen (H_2) and H_2O may remain on the rear-side surface of Si substrate. The blisters which form at the Si/ Al_2O_3 interface occur under an external load in the presence of a tensile residual stress due to the effusion of H_2 and H_2O [11]. The blistering may deteriorate minority carrier lifetime. Several studies have claimed that treating the Al_2O_3 films with enough thermal budgets prior to the capping of $\text{SiN}_x\text{:H}$ and thinning the thickness Al_2O_3 film are two possible ways to conquer this obstacle [12].

In this study, a non-vacuum spatial ALD with a deposition rate of 10 nm/min which is ten times faster than the traditional ALD systems is developed. The fast-growing Al_2O_3 films are used as a rear-side passivation layer applied to the P-type PERC structure. In the beginning, the analysis of electrical and structural properties for pure Al_2O_3 is characterized. The expected blistering formation is observed through an optical microscope. Two approaches tried to solve the blistering problem as well as to improve the efficiency of PERC. Firstly, a very thin stoichiometric silicon dioxide (SiO_2) film deposited by inductively coupled plasma chemical vapor deposition (ICPCVD) is inserted into the interface between Al_2O_3 and silicon wafer to reduce blisters. In the meantime, SiO_2 film can further chemically passivate the interface defects. Secondly, reducing the thickness of the Al_2O_3 film to lower than 10 nm and increasing the post-annealing temperature to a higher temperature of 650°C to enhance out diffusion of gas. After that, the $\text{SiN}_x\text{:H}$ films with abundant hydrogen content prepared by ICPCVD are capped on the Al_2O_3 films to enhance the passivation effect by filling dangling bonds. The positive effect of the stacked passivation layer is proven from a quasi-steady-state photo-conductance (QSSPC). The electrical performance for the PERC devices with various rear-side-passivated structures is eventually investigated.

Methods

Few pieces of 15.6 cm × 15.6 cm shiny etched Cz-Si wafers (P-type, 5 Ω-cm, (100-oriented)) wafers of 200 μm thick were prepared. They were then etched in a chemical polishing solution to remove the saw damages at the edges followed by standard RCA clean. Subsequently, the identical Al_2O_3 films were deposited on both sides of the Si wafers to evaluate the passivation effect. Various thicknesses of the Al_2O_3 films from 10 to 25 nm were firstly prepared before sending them to the furnace for

post-annealing process in N_2 ambient. The temperature was set from 450°C to 600°C. We prepared other wafers capped with identical thin SiO_2 films as an interlayer by ICPCVD. The Al_2O_3 films were deposited on the top of SiO_2 films to form stacked structures. Those samples were also annealed in the range from 450°C, 500°C, 550°C, to 600°C, respectively. For a special case, the stacked structures $\text{SiO}_2/\text{Al}_2\text{O}_3$ with thinner Al_2O_3 of about 8 nm were fabricated for comparison. A higher annealing temperature of 650°C was treated on these samples to drive more imbedded gas out diffused. The stacked structures capped with silicon nitride films doped hydrogen ($\text{SiN}_x\text{:H}$) was made by ICPCVD, forming the triple-layer stacked structure of $\text{SiO}_2/\text{Al}_2\text{O}_3/\text{SiN}_x$. These triple-layer stacked films were then annealed at 450°C for 20 min.

High-resolution scanning electrical microscope (HR-SEM) and optical microscope (OM) were used to observe the thicknesses of the Al_2O_3 films and the distribution of blisters, respectively. The wafers were characterized by QSSPC effective lifetime measurement (Sinton Company WCT-120; Sinton Instruments, Boulder, CO, USA). Cross-sectional images of the stacked films were carried out by transmission electron microscope (TEM).

After completing the analysis of passivation effect, we started to fabricate the entire PERC devices. For fabrication of emitter, P-type cleaned wafers were thermal diffused by phosphorous atoms in a quartz tube furnace at 850°C. Anti-reflective coatings (ARCs) were deposited by PECVD. Four kinds of the passivation films were prepared on the rear side of wafers as shown in Figure 1. Cell A has a pure Al_2O_3 film on the rear side of the Si wafer, having a large number of blisters. Cell B has a thin SiO_2 film inserted between the Al_2O_3 film and Si wafer, having fewer blisters compared to sample A. Note that blisters may probably occur at two interfaces of $\text{Al}_2\text{O}_3/\text{SiO}_2$ and SiO_2/Si substrates. According to our experimental results, almost all the blisters are observed to stay at the SiO_2/Si substrate. This phenomenon can be attributed to the fact that the SiO_2 thin films fabricated by ICPCVD have lots of pores, allowing H_2 and H_2O penetrating into the region between the SiO_2 layer and the Si substrate after the deposition of Al_2O_3 . In contrast with cell B, cell C has the same stacked structure, but thinner Al_2O_3 film of 8 nm. Post-annealing at 650°C was performed on it as well. Thus, the blisters in cell C were out-gassed, forming some voids to act as defects. The last cell D has a triple-layer stacked passivation film of $\text{SiO}_2/\text{Al}_2\text{O}_3/\text{SiN}_x\text{:H}$ as described above. The detailed thickness information for each layer is summarized in Table 1. Laser ablation technique was subsequently used to form the local openings to let the aluminum paste contact with the Si wafer through a co-firing process. I-V characteristics of solar cells were measured using AM1.5G (100 mW/cm²) solar simulator.

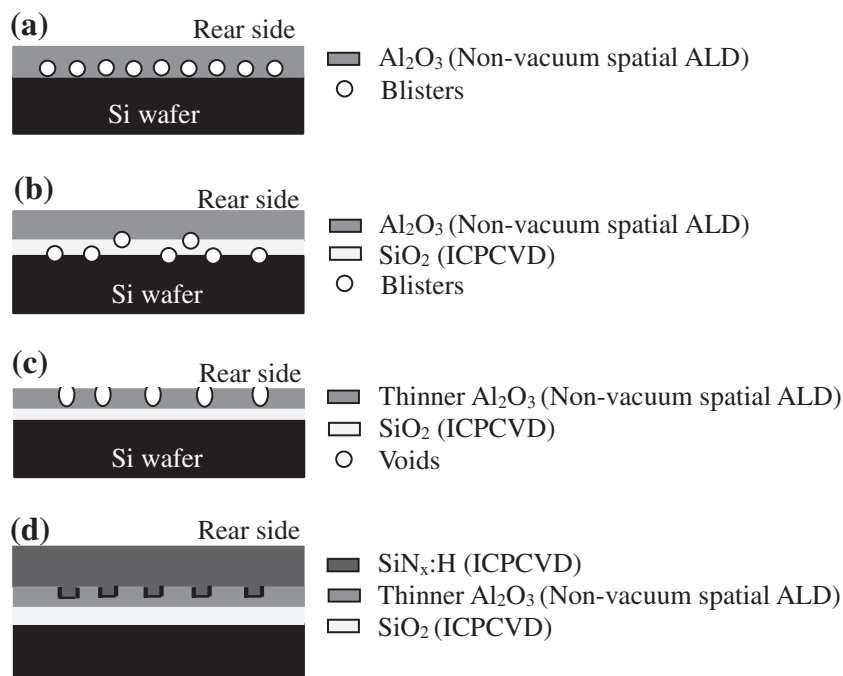


Figure 1 Introduction for four kinds of structure of rear-side passivation films. (a) Cell A has a pure Al₂O₃ film on the rear side of the Si wafer; (b) cell B has a thin SiO₂ film inserted between the Al₂O₃ film and Si wafer; (c) cell C has the same stacked structure to that of cell B, but thinner Al₂O₃ film of 8 nm; and (d) cell D has a triple-layer stacked passivation film of SiO₂/Al₂O₃/SiN_x:H. We introduce the detailed information about the passivation films fabricated in various stages.

Results and discussion

Figure 2a shows the HR-SEM images for various cycles of deposition of the Al₂O₃ films including 50, 100, 300, and 400 cycles. The regime marked by a double-sided arrow is the Al₂O₃ film. The aim of capping the SiN_x film on the Al₂O₃ film is to discriminate each layer to be observed clearly. From this figure, it can be seen that under different deposition cycles, all the Al₂O₃ films are uniform without any rough morphology on the surface, revealing the feasibility and reproducibility of this ALD system. Thicknesses of 10.3, 34.8, 48.8, and 62.6 nm correspond to 50, 200, 300, and 400 cycles, respectively. The ALD process allows the deposition of Al₂O₃ films with an accurate thickness control is demonstrated in Figure 2b. It is shown that the Al₂O₃ film thickness scales near linear with the number of ALD cycles for

our non-vacuum spatial ALD. The slope in Figure 2b is defined as growth per cycle (GPC). The GPC here is around 0.16 nm/cycle, 1 s per cycle, so that the deposition rate is around 10 nm/min. Compared to traditional plasma-enhanced ALD and thermal ALD, the deposition rate of 10 nm/min is much faster, displaying its high potential for being used in the industrials.

The recombination rate at the Si wafer surface is normally controlled by the excess concentration of minority carriers near the surface. Minimizing the concentration of minority concentration thus reduces the surface recombination rate. Figure 3 shows the minority carrier lifetime for various Al₂O₃ film thicknesses with 10 to 25 nm annealed at 450°C to 600°C in the N₂ ambient. As can be seen in Figure 3, the trends of lifetime for all curves are almost the same, increasing with the increase of temperature firstly and decreasing after at the annealing temperature of 500°C. The decreased lifetime after 500°C can be explained that little bonding structure is broken, releasing few dangling bonds to trap minority carriers. On the other hand, as the thickness of the Al₂O₃ film increases, the minority carrier lifetime increases as well. This can be attributed to a lower interface defect density deduced from capacitance voltage measurement for a thicker Al₂O₃ film [13]. The peak lifetime 85.5 μs is achieved (the lifetime of bare wafer is

Table 1 Detailed thickness information of rear-side passivation films

Cell type	SiO ₂ (nm)	Al ₂ O ₃ (nm)	SiN _x :H (nm)	Annealing temperature prior to cap SiN _x :H (°C)
A	N/A	25	N/A	500
B	3	25	N/A	500
C	3	8	N/A	650
D	3	8	70	650

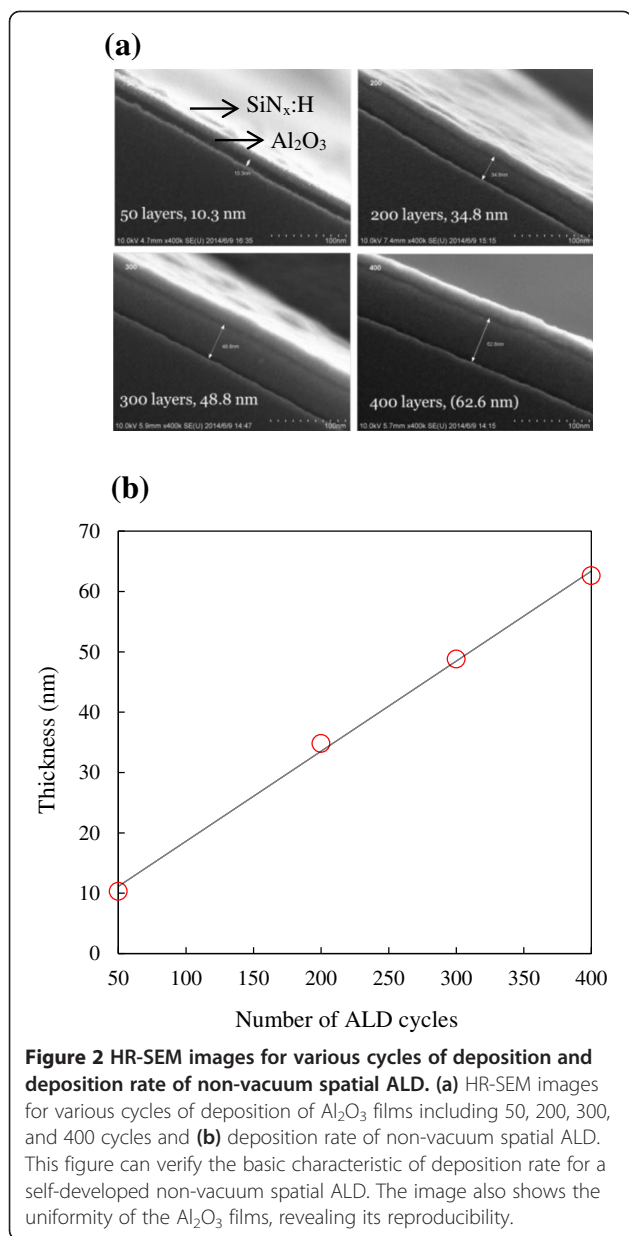


Figure 2 HR-SEM images for various cycles of deposition and deposition rate of non-vacuum spatial ALD. **(a)** HR-SEM images for various cycles of deposition of Al₂O₃ films including 50, 200, 300, and 400 cycles and **(b)** deposition rate of non-vacuum spatial ALD. This figure can verify the basic characteristic of deposition rate for a self-developed non-vacuum spatial ALD. The image also shows the uniformity of the Al₂O₃ films, revealing its reproducibility.

about 5 μ s), while the thickness of the Al₂O₃ film is 25 nm and the annealing temperature is 500°C.

In most cases, blister formation caused by the effusion of H₂O and H₂ from the silicon bulk may occur upon post-annealing step. Those unwanted blisters are regarded as defects, deteriorating both the chemical effect and field effect of the Al₂O₃ films [14]. Figure 4 displays the optical microscope images for different thicknesses of the Al₂O₃ film annealed at 500°C: (a) 10 nm, (b) 15 nm, (c) 20 nm, and (d) 25 nm. All the samples have a large number of blisters shown as little spots highlighted by a circle symbol. The diameters of the blister are uniform in the range of 3~4 μ m. With the increase of

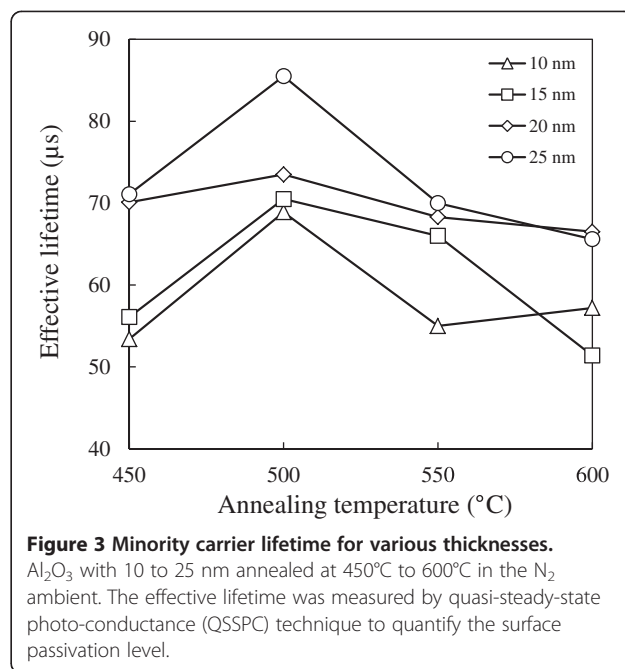


Figure 3 Minority carrier lifetime for various thicknesses.

Al₂O₃ with 10 to 25 nm annealed at 450°C to 600°C in the N₂ ambient. The effective lifetime was measured by quasi-steady-state photo-conductance (QSSPC) technique to quantify the surface passivation level.

thickness, the blister density goes lower, resulting in a better passivation effect. The phenomenon can be explained in terms of two aspects: (i) as the Al₂O₃ films deposited layer by layer, the weight of entire films becomes heavier, making the blister under the Al₂O₃ films dissipate literally; (ii) one Al₂O₃ layer forms via the reaction between TMA and H₂O in sequence on the surface of the silicon wafer. After dozens of cycles, the chemical reaction tends to be stable. The usage of H₂O raises due to its up and down movement among each porous Al₂O₃ layer and chemical reaction with residual TMA at the bottom of the Al₂O₃ films. Hence, the amount of the blisters decreases with an increase of the thickness of the Al₂O₃. Simultaneously, the distribution of blisters can also be an evidence to account for the lifetime trend in Figure 3.

The blister-blocking effect of SiO₂ on silicon can be reflected in Figure 5. Figure 5a shows the minority carrier lifetime for 3 nm of the SiO₂ films capped with various Al₂O₃ films thicknesses of 10 to 25 nm annealed at 450°C to 600°C in the N₂ ambient. Compared to the trend of Figure 3, it almost maintains unchanged, but the average lifetime of all samples has a little increase. The peak value of 107.2 μ s is obtained still when the thickness of the Al₂O₃ film is 25 nm, and the annealing temperature is 500°C. The increase of 21.7 μ s between two peak lifetime values can be attributed to the enormous reduction of blisters, as shown in Figure 5b. The major reason to support SiO₂ film to be our option is that the SiO₂ film has more stoichiometric configuration compared to native oxide (SiO_x). When the Al₂O₃ films

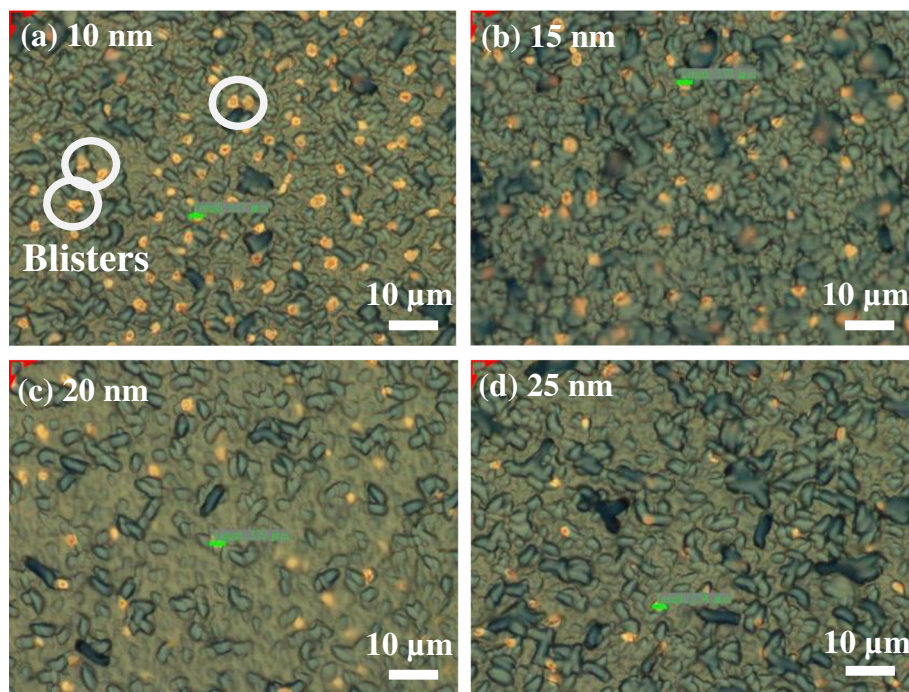


Figure 4 Optical microscope images for different thicknesses of Al_2O_3 film annealed at 500°C . (a) 10 nm, (b) 15 nm, (c) 20 nm, (d) 25 nm.

deposited directly on the silicon substrate without SiO_2 films as interlayers, the oxygen atom of reactant H_2O tends to bond with SiO_x to form the stable SiO_2 ; thus, the released H_2 and residual H_2O may probably become the blisters after post-annealing process. The highly stoichiometric ICPCVD- SiO_2 films inserted into the interface between the Al_2O_3 and silicon wafer effectively prevent the considerable amount of blisters from occurring. In addition, several studies have claimed that SiO_2 film is a good candidate for chemical passivation to eliminate the dangling bonds on the surface of silicon wafer [15,16]. Also, it can help the Al_2O_3 films to rearrange their negative fixed charge distributed near the $\text{SiO}_2/\text{Al}_2\text{O}_3$ interface [17,18].

For further improvement for the blistering problem, we reduce the thickness of Al_2O_3 to lower than 10 nm and increase the annealing temperature to 650°C , giving an enough thermal budget prior to the capping of the $\text{SiN}_x:\text{H}$ film. The out-gassing phenomenon can be found. Here, the blister number can further decrease, approaching near blister free. Some voids existing within the Al_2O_3 film are caused by the out-gassing effusion. However, the subsequent deposition of $\text{SiN}_x:\text{H}$ prepared by ICPCVD would provide abundant hydrogen atoms to fill the dangling bonds via the voids. The post-anneal (450°C for 20 min) performed after the deposition of $\text{SiN}_x:\text{H}$ is able to activate the passivation of the triple-layer stacked structure [19]. Figure 6 shows the injection

level dependent minority carrier lifetime for the stacked passivation film of $\text{Si}/3\text{ nm-SiO}_2/8\text{ nm-Al}_2\text{O}_3/70\text{ nm-SiN}_x:\text{H}$ film and of $\text{Si}/3\text{ nm-SiO}_2/6\text{ nm-Al}_2\text{O}_3/70\text{ nm-SiN}_x:\text{H}$ film. The effective lifetime is calculated from the photoluminescence intensity by the self-consistent calibration method proposed by Trupke et al. [20]. Both the triple-layer stacked films have the same structure except the thickness of the Al_2O_3 film. The former one has a higher average lifetime of $315\ \mu\text{s}$ compared to the latter one of $147\ \mu\text{s}$. Two major factors, negative fixed charge and blisters, are found to influence the lifetime of the Al_2O_3 films. Generally, reducing the thickness of the Al_2O_3 films to lower than 10 nm and increasing a post-annealing temperature to higher than 650°C can make blisters out-gassed. In this case, both 6- and 8-nm Al_2O_3 films are blister free, indicating the lifetime is determined only by negative fixed charge. According to our previous research and some references [21,22], the negative fixed charge may accumulate to enhance the passivation effect as the thickness increases. Hence, the sample with an 8-nm-thick Al_2O_3 layer has a higher lifetime, displaying stronger field-effect passivation than the sample with a 6-nm-thick Al_2O_3 layer. The optimized lifetime of $315\ \mu\text{s}$ is about three times higher than $107.2\ \mu\text{s}$ of the stacked film without $\text{SiN}_x:\text{H}$. Note that the thickness of the Al_2O_3 within the triple-layer stacked film is reduced to lower than 10 nm, decreasing its field-effect passivation. However, according to some investigation of

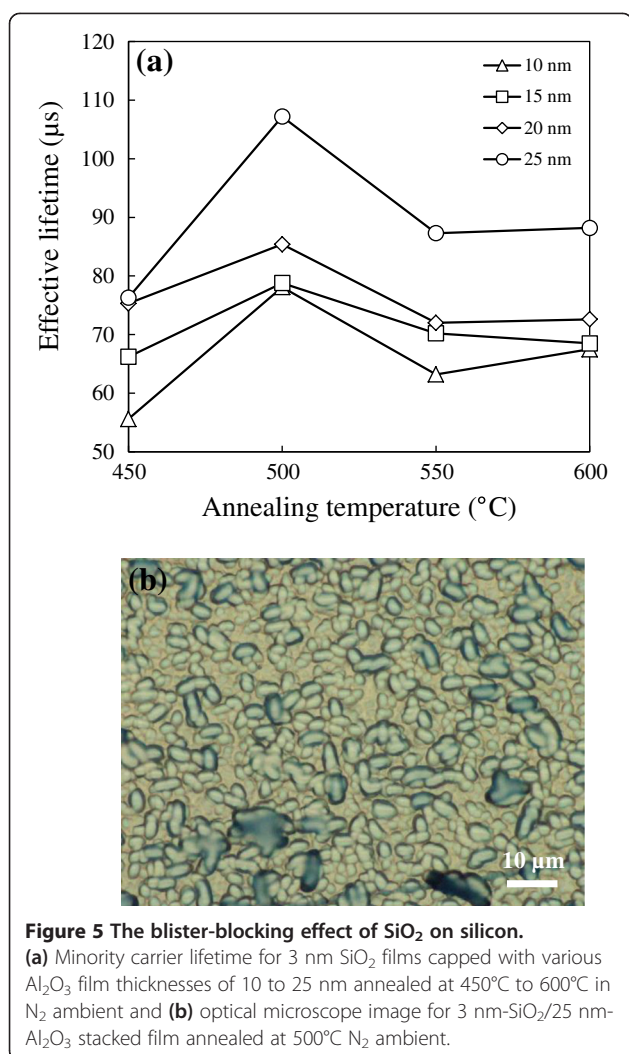


Figure 5 The blister-blocking effect of SiO₂ on silicon. **(a)** Minority carrier lifetime for 3 nm SiO₂ films capped with various Al₂O₃ film thicknesses of 10 to 25 nm annealed at 450°C to 600°C in N₂ ambient and **(b)** optical microscope image for 3 nm-SiO₂/25 nm-Al₂O₃ stacked film annealed at 500°C N₂ ambient.

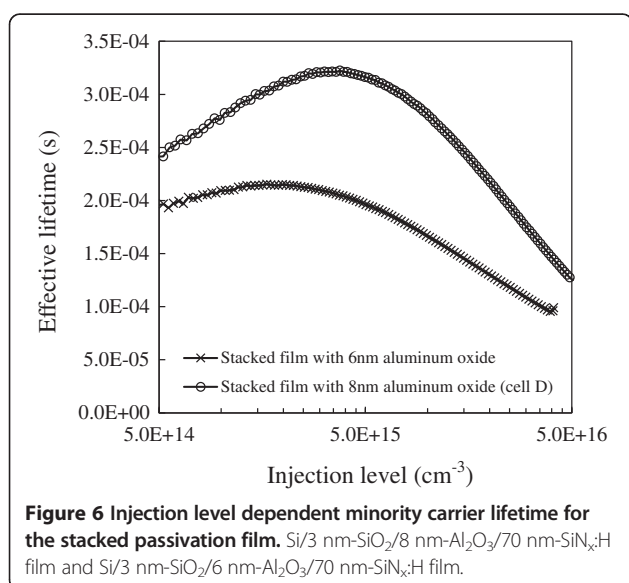


Figure 6 Injection level dependent minority carrier lifetime for the stacked passivation film. Si/3 nm-SiO₂/8 nm-Al₂O₃/70 nm-SiN_x:H film and Si/3 nm-SiO₂/6 nm-Al₂O₃/70 nm-SiN_x:H film.

[23–26], they demonstrate that a thin Al₂O₃ of about 10 nm is still sufficient for providing an excellent level of surface passivation. Despite the field-effect passivation may become weaker in this case, the chemical passivation from SiN_x:H dominates the whole performance strongly. For a short summary, hydrogen atom indeed plays a critical role in combining with the Al₂O₃ film as the passivation stacks.

Figure 7 displays the high-resolution transmission electron microscope (HR-TEM) cross-sectional image of the stacked Si/3 nm-SiO₂/8 nm-Al₂O₃/70 nm-SiN_x:H film, in which we can see the three interfaces such as Si/SiO₂, SiO₂/Al₂O₃, and Al₂O₃/SiN_x:H are all flattened without any vacancy or void to deteriorate the passivation effect. The very thin SiO₂ film with only 3 nm is deposited using the ICPCVD. The accurate control in thickness is based on the deposition rate determined by the past experiments. In the meanwhile, this TEM image confirms that the Al₂O₃ film deposited by self-developed non-vacuum spatial ALD is quite uniform.

Figure 8 shows the reproducible illuminated I-V curves and performance of PERC cells for the four kinds of rear-side passivation structure including cell (A) pure 25 nm-Al₂O₃ film, (B) 3 nm-SiO₂/25 nm-Al₂O₃ stacked film, (C) 3 nm-SiO₂/8 nm Al₂O₃ film without capping SiN_x:H treated with an annealing temperature of 650°C, and (D) 3 nm-SiO₂/8 nm Al₂O₃ film/70 nm-SiN_x:H treated with an annealing temperature of 450°C for 20 min after the capping of SiN_x:H. All the detailed external parameters are summarized in Table 2. We can find that the electrical performance of cells A and B are almost the same, only with a slight difference in open-circuit voltage (V_{oc}). To understand the performance V_{oc} , we investigate the behavior of minority carrier lifetime of the P-type Si wafer. B. Michl et al. have claimed that the excess carrier lifetime substantially affects the

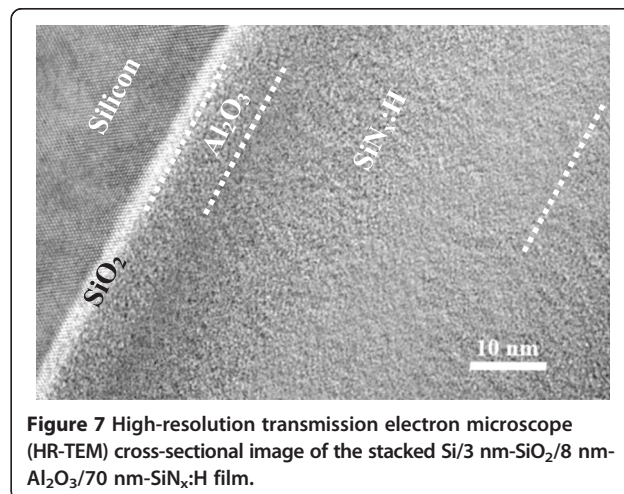
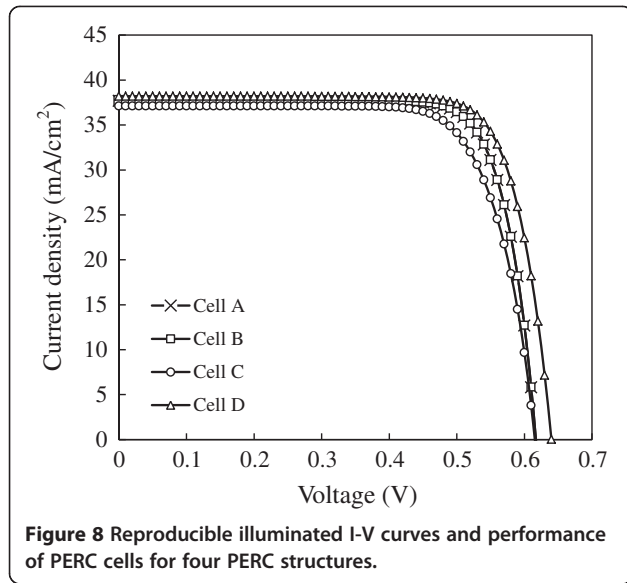


Figure 7 High-resolution transmission electron microscope (HR-TEM) cross-sectional image of the stacked Si/3 nm-SiO₂/8 nm-Al₂O₃/70 nm-SiN_x:H film.



V_{oc} in multi-crystalline materials [27]. Three equations which can describe the relation between minority carrier lifetime and V_{oc} can be expressed by:

$$V_{oc} = \frac{kT}{q} \ln \left(\frac{J_{sc}}{J_{os} + J_{ob}} + 1 \right) \quad (1)$$

$$J_{ob} = q \frac{n_i^2}{N_A} \frac{D_n}{(W_p - X_p)} \left[1 + \frac{D_n / (W_p - X_p)}{S_{back}} \right]^{-1} \quad (2)$$

$$\frac{1}{\tau_{eff}} = \frac{1}{\tau_{bulk}} + \frac{S_{front} + S_{back}}{W} \quad (3)$$

where J_{oe} and J_{ob} are the reverse saturation current, respectively. N_A is doping concentration, n_i is the intrinsic carrier concentration, S_{back} is the recombination velocity of back side surface, and τ_{eff} and τ_{bulk} are effective lifetime and bulk lifetime of devices, respectively. By Equation 3, we can obtain that S_{back} may decrease with the increase of effective lifetime. Whereas the smaller S_{back} leads to a lower J_{ob} expressed in Equation 2. Generally, the value of J_{ob} changes its order of magnitude,

leading to a huge variation of V_{oc} . Hence, from Equation 1, an increased V_{oc} can be obtained by a reduced J_{ob} . The deposition of very thin SiO_2 film in cell B can not only reduce the blister number but also help to rearrange the negative fixed charge near the surface of the Al_2O_3 film, thus improving the minority carrier lifetime. According to the explanation above, the higher lifetime of cell B leads to a higher V_{oc} . As for cell C, it can be seen that all the electrical performances are the worst, especially in fill factor (FF). The factor to influence FF in a solar diode is the contact resistance between metal and semiconductor [28,29]. The blisters in cell C are almost out-gassed, resulting in random distribution of voids. After the laser ablation for the rear contact fabrication, the non-uniform openings can be obtained, forming an unfavorable rear contact. The following high series contact may bring a huge reduction in FF. In comparison with cells A, B, and C, cell D has the apparent improvement in V_{oc} and short-circuit current (J_{sc}). The triple-layer stacked film combines the chemical passivation with field-effect passivation at the same time, leading to a relatively high lifetime of 315 μs . Thus, an optimized V_{oc} can be acquired. As to the high J_{sc} , this can be explained that an optimized rear-side triple-layer stacked passivation also acts as an excellent internal back side reflective coating. By reflecting more long-wavelength light, there is an obvious gain in J_{sc} [30]. The final optimal efficiency of the cell D achieves 19.18%.

Conclusions

In this study, the uniform Al_2O_3 films with high reproducibility are fabricated by self-developed non-vacuum spatial ALD system. We report two effective ways to improve the blistering problem upon the annealing after the deposition of Al_2O_3 , including (i) depositing a thin stoichiometric SiO_2 film on the surface of the silicon wafer by ICPCVD and (ii) further reducing the thickness of the Al_2O_3 film to below 10 nm and provide higher thermal budget to the stacked $\text{Si}/\text{SiO}_2/\text{Al}_2\text{O}_3$ film prior to capping with $\text{SiN}_x\text{:H}$. An obvious improvement on blistering issue can be verified from OM images and minority carrier lifetime measurement. The blisters can be out-gassed when treating the 8-nm thin Al_2O_3 film with a 650°C annealing temperature. The subsequent deposition of 70 nm- $\text{SiN}_x\text{:H}$ film can not only protect the Al_2O_3 film from damage but also provide an effective chemical passivation on the surface of the silicon wafer via the voids. The improved triple-layer stacked $\text{Si}/3 \text{ nm-SiO}_2/8 \text{ nm-Al}_2\text{O}_3/70 \text{ nm-SiN}_x\text{:H}$ passivation film is successfully applied to PERC device with distinct gains in V_{oc} of about 0.03 V and in J_{sc} of about 0.6 mA/cm^2 . The final optimal conversion efficiency of 19.18% for the PERC device with the improved stacked passivation film is obtained.

Table 2 Photovoltaic performance for PERC cells with various rear-side passivation films

Cell type	V_{oc} (V)	J_{sc} (mA/cm^2)	FF	Efficiency (%)
A	0.619	37.6	0.78	18.15
B	0.623	37.7	0.782	18.36
C	0.618	37.2	0.748	17.2
D	0.647	38.2	0.776	19.18

Abbreviations

ARC: anti-reflective coatings; ALD: atomic layer deposition system; CVD: chemical vapor deposition system; FF: fill factor; GPC: growth per cycle; HR-SEM: high-resolution scanning electron microscopy; HR-TEM: high-resolution transmission electron microscope; ICP-CVD: inductively coupled plasma chemical vapor deposition; LPD: liquid-phase deposition technique; V_{oc} : open-circuit voltage; PERC: passivated emitter and rear cell; PVD: physical vapor deposition system; QSSPC: quasi-steady-state photo-conductance; J_{sc} : short-circuit current; TEM: transmission electron microscope.

Competing interests

The authors declare that they have no competing interests.

Authors' contributions

SYL led the experimental and analytical efforts on the passivation effect of various stacked passivation films of PERC. CHY assisted in optimizing the performance of various stacked passivation films and drafted the manuscript. KCW assisted in fabricating the complete PERC. CYK contributed to the design and analysis of the experiments for the stacked passivation films and integrated the comments from all authors. All authors read and approved the final manuscript.

Authors' information

SYL is currently an Associate Professor in the Department of Materials Science and Engineering, DaYeh University, Changhua, Taiwan. He has done work in the field of solar cell materials by plasma-enhanced chemical vapor deposition and hot-wire chemical vapor deposition. CHY is presently a Ph.D. student at the Department of Electrical Engineering, National Chung Hsing University, Taichung, Taiwan, R.O.C., majoring high-efficiency mono-crystalline silicon solar cells. KCW is the leader of Crystalline Silicon R & D. Section, Mosel Vitelic Inc., Taiwan, R.O.C. CYK received the Ph.D. degree from the Department of Materials Science and Engineering, Northwestern University, Evanston, IL, USA in 1978. He has been working as staff scientist in Lawrence Berkeley Laboratory for 2 years and ITRI Hsinchu, Taiwan for 4 years. Currently, he is a Professor in the Department of Electrical Engineering, National Chung Hsing University, Taiwan. His research interests include the synthesis and application of semiconductor materials.

Acknowledgements

This work is sponsored by Mosel Vitelic Inc., Taiwan, R.O.C. and the Ministry of Science and Technology of the Republic of China under the grants No. 102-2221-E-212-021-MY2 and Hsinchu Science Park Bureau, Ministry of Science and Technology, Republic of China under the grants No. 102A24.

Author details

¹Department of Materials Science and Engineering, DaYeh University, No. 168, Xuefu Road, Changhua 515, Taiwan. ²Department of Electrical Engineering, National Chung Hsing University, 250 State Road, Taichung 402, Taiwan. ³Crystalline Silicon R & D Section, Mosel Vitelic Inc, No. 1, Creation Road 1, Hsinchu 300, Taiwan.

Received: 16 November 2014 Accepted: 5 February 2015

Published online: 28 February 2015

References

- Li TA, Ruffell S, Tucci M, Mansoulie' Y, Samundsett C, Delullis S, et al. Influence of oxygen on the sputtering of aluminum oxide for the surface passivation of crystalline silicon. *Sol Energ Mat Sol C*. 2011;95:69–72.
- Maruyama T, Nakai T. Aluminum oxide thin films prepared by chemical vapor deposition from aluminum 2-ethylhexanoate. *Appl Phys Lett*. 1991;58:2079–80.
- Klein TM, Niu D, Epling WS, Li W, Maher DM, Hobbs CC, et al. Evidence of aluminum silicate formation during chemical vapor deposition of amorphous Al_2O_3 thin films on Si (100). *Appl Phys Lett*. 1999;75:4001–3.
- Tristant P, Ding Z, Trang Vinh QB, Hidalgo H, Jauberteau JL, Desmaison J, et al. Microwave plasma enhanced CVD of aluminum oxide films: OES diagnostics and influence of the RF bias. *Thin Solid Films*. 2001;390:51–8.
- Sun J, Sun YC. Chemical liquid phase deposition of thin aluminum oxide films. *Chinese J Chem*. 2004;22:661–7.
- Basu S, Singh PK, Huang JJ, Wang YH. Liquid-phase deposition of Al_2O_3 thin films on GaN. *J Electrochem Soc*. 2007;154:H1041–6.
- Hoex B, Schmidt J, Bock R, Altermatt PP, van de Sanden MCM, Kessels WMM. Excellent passivation of highly doped p-type Si surfaces by the negative-charge dielectric Al_2O_3 . *Appl Phys Lett*. 2007;91:112107–112107–3.
- Benick J, Hoex B, van de Sanden MCM, Kessels WMM, Schultz O, Glunz SW. High efficiency n-type Si solar cells on Al_2O_3 -passivated boron emitters. *Appl Phys Lett*. 2008;92:253504–253504–3.
- Dueñas S, Castán H, García H, de Castro A, Bailón L, Kukli K, et al. Influence of single and double deposition temperatures on the interface quality of atomic layer deposited Al_2O_3 dielectric thin films on silicon. *Appl Phys Lett*. 2006;99:054902–054902–8.
- Poodt P, Lankhorst A, Roozeboom F, Spee K, Maas D, Vermeer A. High-speed spatial atomic-layer deposition of aluminum oxide layers for solar cell passivation. *Adv Mater*. 2010;22:3564–7.
- Bart V, Hans G, Veerle S, Ingrid DW, Johan M, Shuji T, et al. A study of blister formation in ALD Al_2O_3 grown on silicon. In: *PVSC'38: 38th Photovoltaic Specialists Conference IEEE*, June 2012; Austin. Published by IEEE, New York; 2012. 1135–1138
- Hennen L, Granneman EHA, Kessels WMM. Analysis of blister formation in spatial ALD Al_2O_3 for silicon surface passivation. In: *PVSC'38: 38th Photovoltaic Specialists Conference IEEE*, June 2012; Austin. Published by IEEE, New York; 2012. 1049–1054
- Saint-Cast P, Heo YH, Billot E, Olwa P, Hofmann M, Rentsch J, et al. Variation of the layer thickness to study the electrical property of PECVD Al_2O_3 /c-Si interface. *Energy Procedia*. 2011;8:642–7.
- Saint-Cast P, Kania D, Heller R, Kuehnhold S, Hofmann M, Rentsch J, et al. High-temperature stability of c-Si surface passivation by thick PECVD Al_2O_3 with and without hydrogenated capping layers. *Appl Surf Sci*. 2012;258:8371–6.
- Sameshima T, Sakamoto K, Tsunoda Y, Saitoh T. Improvement of SiO_2 properties and silicon surface passivation by heat treatment with high-pressure H_2O vapor. *Jan J Appl Phys*. 1998;37:L1452–4.
- Schmidt J, Kerr M, Cuevas A. Surface passivation of silicon solar cells using plasma-enhanced chemical-vapour-deposited SiN films and thin thermal SiO_2 /plasma SiN stacks. *Semicond Sci Technol*. 2001;16:164–70.
- Agostinelli G, Delabie A, Vitanov P, Alexieva Z, Dekkers HFW, Wolf SD, et al. Very low surface recombination velocities on p-type silicon wafers passivated with a dielectric with fixed negative charge. *Sol Energ Mat Sol C*. 2006;90:3438–43.
- Gielis JJH, Hoex B, van de Sanden MCM, Kessels WMM. Negative charge and charging dynamics in Al_2O_3 films on Si characterized by second-harmonic generation. *J Appl Phys*. 2008;104:073701–073701–5.
- Dingemans G, van de Sanden MCM, Kessels WMM. Excellent si surface passivation by low temperature SiO_2 using an ultrathin Al_2O_3 capping film. *Phys Status Solidi-R*. 2011;5:22–4.
- Trupke T, Bardos RA, Abbott MD. Self-consistent calibration of photoluminescence and photoconductance lifetime measurements. *Appl Phys Lett*. 2005;87:184102–184102–3.
- Boris V, Florian W, Dimitri Z, Rolf B, Jan S. Comparison of the thermal stability of single Al_2O_3 layers and Al_2O_3/SiN_x stacks for the surface passivation of silicon. *Energy Procedia*. 2011;8:307–12.
- Teng YW, Cheng CL, Chien HH, Chen HD, Chung YK. Effect of annealing on aluminum oxide passivation layer for crystalline silicon wafer. *J Energy Power Eng*. 2013;7:1505–10.
- Black LE, Allen T, McIntosh KR, Cuevas A. Effect of boron concentration on recombination at the p-Si- Al_2O_3 interface. *Appl Phys Lett*. 2014;115:093707–093707–9.
- Duttgupta S, Lin F, Shetty KD, Wilson M, Ma FJ, Lin JJ, et al. State-of-the-art surface passivation of boron emitters using inline PECVD AlO_x/SiN_x stacks for industrial high-efficiency silicon wafer solar cells. In: *PVSC'38: 38th Photovoltaic Specialists Conference IEEE*, June 2012; Austin. Published by IEEE, New York; 2012. 1036–1039
- Wu J, Liu YY, Wang XS, Zhang LJ. Application of ion implantation emitter in PERC solar cells. *IEEE J Photovoltaics*. 2014;4:52–7.
- Hoex B, Gielis JJH, van de Sanden MCM, Kessels WMM. On the c-Si surface passivation mechanism by the negative-charge-dielectric Al_2O_3 . *J Appl Phys*. 2008;104:113703–113703–7.
- Michl B, Rüdiger M, Giesecke JA, Hermle M, Warta W, Schubert MC. Efficiency limiting bulk recombination in multicrystalline silicon solar cells. *Sol Energ Mat Sol C*. 2012;98:441–7.

28. Gatz S, Dullweber T, Brendel R. Evaluation of series resistance losses in screen-printed solar cells with local rear contacts. *IEEE J Photovoltaics*. 2011;1:37–42.
29. Meier DL, Good EA, Garcia RA, Bingham BL, Yamanaka S, Chandrasekaran V, et al. Determining components of series resistance from measurements on a finished cell. In: *Photovoltaic Energy Conversion, Conference Record of the 2006 IEEE 4th World Conference on (Volume 2)*, May 2006; Waikoloa. Published by IEEE, New York; 2006. 1315–1318
30. Lin JW, Chen YY, Gan JY, Hseih WP, Du CH, Chao TS. Improved rear-side passivation by atomic layer deposition $\text{Al}_2\text{O}_3/\text{SiN}_x$ stack layers for high V_{OC} industrial P-type silicon solar cells. *IEEE Electr Device L*. 2013;34:1163–5.

Submit your manuscript to a SpringerOpen[®] journal and benefit from:

- ▶ Convenient online submission
- ▶ Rigorous peer review
- ▶ Immediate publication on acceptance
- ▶ Open access: articles freely available online
- ▶ High visibility within the field
- ▶ Retaining the copyright to your article

Submit your next manuscript at ▶ springeropen.com
